2002

Evaporative Modeling In A Thin-Film Region of Micro-Channel

K. Park
Hanyang University

K. J. Noh
Hanyang University

K. S. Lee
Hanyang University

R10-5

EVAPORATIVE MODELING IN A THIN-FILM REGION OF MICRO-CHANNEL

*Kyoungwoo Park, Ph.D, Research Professor, Center of Innovative Design Optimization Technology, Hanyang University, 17 Haengdang-Dong, Sungdong-Ku, Seoul 133-791, KOREA;
Tel.: 82-2-2290-0478; Fax: 82-2-2291-4070 ; E-Mail: kwoopark@hanyang.ac.kr
*Author for Correspondence

Kwan-Joong Noh, Graduate Student, Hanyang University, 17 Haengdang-Dong, Sungdong-Ku, Seoul 133-791, KOREA;
Tel.: 82-2-2290-0426; Fax: 82-2-2295-9021: E-Mail: ssawar@kebi.com

Kwan-Soo Lee, Ph.D, Professor, School of Mechanical Engineering, Hanyang University, 17 Haengdang-Dong, Sungdong-Ku, Seoul 133-791, KOREA;
Tel.: 82-2-2290-0426; Fax: 82-2-2295-9021; E-Mail: ksleehy@hanyang.ac.kr

ABSTRACT

A mathematical model which can be predicted the flow and heat transfer characteristics for evaporating thin film region in micro channel is presented and an analytical investigation is performed by using the presented model. For the formulation of modeling, the flow of the vapor phase and the shear stress at the liquid-vapor interface are considered. In addition, the disjoining pressure and the capillary force which drive the liquid flow at the liquid-vapor interface in thin film region are adopted. Comparing the magnitude of capillary and disjoining pressures, the length of thin film region can be calculated. Results show that the influence of variation of vapor pressure on the liquid film flow is not negligible. It is also found that as the heat flux increases, the length of thin film region and the film thickness decrease and the local evaporative mass flux increases linearly.

NOMENCLATURE

In text

INTRODUCTION

For the reliability, high performance, and compactness of electronic devices, the technologies for dissipating the generated heat in electronic devices have been proposed and developed. Among them, the use of phase-change technique to enhance the heat transfer has been paid attention in chemical processing equipment and nuclear reactor as well as electronic cooling. The capillary heat pumps such as capillary pumped loop (CPL) system and heat pipes have been used successfully for this application. Recently, the advancement of packaging technology has led to the miniaturization (i.e. the hydraulic diameter of these devices is on the order of 100-300μm) and the increasing in density of electronics component. Therefore, it becomes more important to remove the generated heat in micro-scale devices. The micro-CPL system consists of the evaporator, condenser, vapor and liquid lines and can be applicable to the small-scale device that uses phase change to transfer thermal energy and it belongs to the application of MEMS (micro-electro-mechanical systems). When a liquid contacts a solid surface, the extended meniscus is divided into three parts; (1) the intrinsic meniscus region which is dominated by the capillary forces, (2) the evaporating thin film region which is governed by the combined effects of both capillary and disjoining pressure, and (3) the adsorbed region where the evaporation doses not occur. Among these three parts, the thin film region where the majority of heat is transferred may be the most important region.

Many efforts have been devoted to establishing the analytical models and conducting the experiments for the performance of the extended meniscus on a flat plate for last two decades.

Derjaguin et. al. (1965) established first the analysis of the thermo-fluid characteristics in the evaporating thin film region and showed that the effect of the solid-liquid molecular interactions on the liquid in the thin film was a pressure reduction relative to the vapor pressure in equilibrium with the thin film. Potash and Wayner (1972) studied the transport processes occurring in an evaporating extended meniscus in view of the physicochemical phenomena. They said that the liquid flows by both disjoining pressure and a change in the meniscus curvature provided the necessary pressure gradient. Mirzamoghadam and Catton (1988) investigated analytically the transport phenomena to obtain the shape of an evaporating meniscus attached to an inclined heated plate. They derived the meniscus profile by using an appropriate liquid film velocity and temperature distribution in an integral approach method. Xu and Carey (1990) conducted a combined analytical and experimental investigation of the liquid flow behavior in V-shaped microgrooves. They suggested an analytical model that predicted the heat transfer characteristics of film evaporation and found that the disjoining pressure differences may play a central role in evaporation processes. Swanson and Herdt (1992) formulated the evaporating meniscus in a capillary tube by considering the Young-Laplace equation, Marangoni convection, London-van der Waals dispersion forces, and non-equilibrium interface conditions. They found that the effect of the dispersion number (A) on the meniscus profile was very large and the liquid pressure difference increased with increasing dispersion number. Schonberg and Wayner (1992) developed an analytical model that introduced the concept of an integral heat sink. They showed that the thin film curvature approached a constant asymptotic value of the thin film joined the meniscus. Ha and Peterson (1996) developed a theoretical model for the heat transfer characteristics of the evaporating thin liquid films in V-shaped microgrooves with non-uniform input heat fluxes. The result showed that when the dispersion number and the superheat are constant, the main factor affecting the length of the evaporating interline region is the heat flux supplied to the bottom of the plate. Kobayashi et. al. (1996) investigated the evaporative heat and mass transfer phenomena in the vicinity of the liquid meniscus edge in the evaporator of a groove heat pipe theoretically and experimentally. The result showed that a large heat flux is transported in the narrow micro-region.

As stated above, a number of investigations have been conducted on this region because the high heat transport rates are occurred in the process of evaporating thin film. However, most of these works neglected the effect of vapor flow (i.e. the vapor pressure was assumed to be constant) and some of them ignored the disjoining pressure effect also. The objectives of this work are to obtain the new mathematical modeling of thin film region of evaporator and to investigate the effect of the applied heat on the flow and heat transfer characteristics. The results of this work can be used as a fundamental data in design of the micro scale evaporator.

MATHEMATICAL MODELING

The geometrical configuration and the coordinate system for the evaporating thin film flow in a micro parallel plate are shown in Fig. 1. As the majority of the heat transfer is occurred at the thin film region due to the very thin thickness, we focus on this region for the predicting of flow and thermal characteristics. As shown in Fig. 1, we only consider the one-half of parallel plate for calculation because of the geometric symmetry. The following assumptions are employed in the derivation of the governing equations.

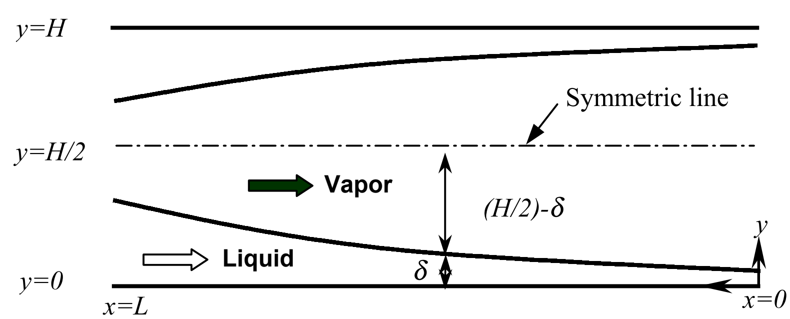

Fig. 1 Geometry and coordinate systems for thin film region of evaporator

- Steady-state, two-dimensional laminar flow

- Incompressible for liquid and vapor flows
- The convective terms are negligible because the flow is very slow.
- Constant fluid properties and surface tension
- Occurring the evaporation in the thin-film region

In the thin film region, the pressure difference between vapor and liquid phases($P_v - P_l$) is due to both capillary and disjoining pressure effects and can be expressed as

$$P_v - P_l = \frac{\overline{A}}{\delta^3} + \sigma K \tag{1}$$

where P_v and P_l represent the vapor pressure and the liquid pressure, respectively. $\overline{A}$ is a dispersion constant and specified here as a positive value [Schonberg and Wayner (1992)] and δ is the film thickness. σ and K are the surface tension and the curvature, respectively. The first term on the right hand side of Eq. (1) is the disjoining pressure which prevents evaporation and the second term expresses the capillary pressure due to interfacial curvature. The curvature of the interface is a function of film thickness and can be expressed as

$$K = \frac{d^2\delta}{dx^2}\left[1 + \left(\frac{d\delta}{dx}\right)^2\right]^{-1.5} \tag{2}$$

Combining Eqs. (1) and (2), assuming constant surface tension, and differentiating it with respect to x yields

$$\frac{d^3\delta}{dx^3} - 3\left(\frac{d\delta}{dx}\right)\left(\frac{d^2\delta}{dx^2}\right)^2\left[1 + \left(\frac{d\delta}{dx}\right)^2\right]^{-1} - \frac{1}{\sigma}\left(\frac{dP_v}{dx} - \frac{dP_l}{dx} + \frac{3\overline{A}}{\delta^4}\frac{d\delta}{dx}\right)\left[1 + \left(\frac{d\delta}{dx}\right)\right]^{-1.5} = 0 \tag{3}$$

As can be seen in Eq. (3), in order to calculate the film thickness, δ , first the liquid and vapor pressures must be obtained.

The conservative momentum equation for steady-state, laminar, incompressible flow can be expressed as a tenser form

$$\frac{\partial}{\partial x_j}\left(\rho u_i u_j\right) = -\frac{\partial P}{\partial x_i} + \frac{\partial}{\partial x_j}\left(\mu \frac{\partial u_i}{\partial x_j}\right) + S \tag{4}$$

where u is the velocity and S denotes the source term.

The momentum equation for the liquid in the thin film region can be approximated by the lubrication theory of fluid mechanics and its boundary conditions are no-slip condition at the wall and shear stress condition at the liquid-vapor interface. The boundary conditions can be written as

$$u_l\big|_{y=0} = 0, \quad \left.\frac{\partial u_l}{\partial y}\right|_{y=\delta} = -\frac{\tau_i}{\mu_l} \tag{5}$$

where the subscript l denotes the liquid-phase and τ_i is the shear stress at the liquid-vapor interface. From the above two equations, we obtain the liquid velocity profile for x-direction:

$$u_l = -\frac{1}{2\mu_l}\left(\frac{dP_l}{dx}\right)(2\delta y - y^2) - \frac{\tau_i}{\mu_l} y \tag{6}$$

By the definition of mass flow rate per unit width, the liquid mass flow rate (Note that the liquid mass flow rate is one-half of the total liquid mass flow rate), $\dot{m}_l'(x)$, can be obtained from Eq. (6) as

$$\dot{m}_l'(x) = \int_0^{y=\delta} \rho_l u_l dy = -\frac{\delta^3}{3\nu_l}\left(\frac{dP_l}{dx}\right) - \frac{\tau_i}{2\nu_l}\delta^2 \tag{7}$$

The momentum equation for the vapor phase can be used in Eq.(4). The liquid velocity at liquid-vapor interface for vapor, $u_{l,i}$, is assumed to flow towards the vapor phase by evaporation and the velocity gradient at symmetric line is set to zero. The boundary conditions are

$$u_v\big|_{y=\delta} = -\frac{\delta^2}{2\mu_l}\left(\frac{dP_l}{dx}\right) - \frac{\tau_i}{\mu_l}\delta, \quad \left.\frac{\partial u_v}{\partial y}\right|_{y=\frac{H}{2}} = 0 \tag{8}$$

where the subscript v is the vapor-phase. From Eqs. (4) and (8), the vapor velocity profile can be obtained

$$u_v = \frac{1}{2\mu_v}\left(\frac{dP_v}{dx}\right)y^2 - \frac{H}{2\mu_v}\left(\frac{dP_v}{dx}\right)y + C \tag{9a}$$

$$C = -\frac{1}{2}\left[\frac{1}{\mu_l}\left(\frac{dP_l}{dx}\right) + \frac{1}{\mu_v}\left(\frac{dP_v}{dx}\right)\right]\delta^2 - \left[\frac{\tau_i}{\mu_l} - \frac{H}{2\mu_v}\left(\frac{dP_v}{dx}\right)\right]\delta \tag{9b}$$

At the liquid-vapor interface, the shear stress for vapor phase is equal to that for liquid phase. Therefore, the vapor shear stress at $y = \delta$ can be expressed as

$$\tau_i = \mu_l \left.\frac{\partial u_l}{\partial y}\right|_{y=\delta} = \mu_v \left.\frac{\partial u_v}{\partial y}\right|_{y=\delta} = \left(\delta - \frac{H}{2}\right)\left(\frac{dP_v}{dx}\right) \tag{10}$$

Substituting Eq. (10) into (9), and noting that by definition, $\dot{m}_v'(x) = \int_\delta^{H/2} \rho_v u_v dy$, the vapor mass flow rate yields

$$\dot{m}_v'(x) = \frac{dP_v}{dx}\left(-\frac{H^3}{24\nu_v} + \frac{\rho_v\delta H^2}{4\mu_l} + \frac{\delta H^2}{4\nu_v} - \frac{\rho_v H\delta^2}{\mu_l} - \frac{H\delta^2}{2\nu_v} + \frac{\delta^3}{3\nu_v} + \frac{\rho_v\delta^3}{\mu_l}\right) + \frac{dP_l}{dx}\left(-\frac{\delta^2 H}{4\mu_l} + \frac{\delta^3}{2\mu_l}\right)\rho_v \tag{11}$$

here $\dot{m}_v'(x)$ is one-half of the total vapor mass flow rate. The pressure gradient for vapor, dP_v/dx, can be expressed in terms of liquid pressure gradient and vapor mass flow rate as follows;

$$\frac{dP_v}{dx} = \left\{\dot{m}_v + \frac{dP_l}{dx}\left(-\frac{\delta^2 H}{4\mu_l} + \frac{\delta^3}{2\mu_l}\right)\rho_v\right\}\Big/ A$$

$$A = -\frac{H^3}{24\nu_v} + \frac{\rho_v\delta H^2}{4\mu_l} + \frac{\delta H^2}{4\nu_v} - \frac{\rho_v H\delta^2}{\mu_l} - \frac{H\delta^2}{2\nu_v} + \frac{\delta^3}{3\nu_v} + \frac{\rho_v\delta^3}{\mu_l} \tag{12}$$

Substituting Eq.(10) into Eq.(7), the pressure gradient for liquid can be obtained.

$$\frac{dP_l}{dx} = \frac{3}{2\delta}\left(\delta - \frac{H}{2}\right)\frac{dP_v}{dx} - \frac{3\nu_l}{\delta^3}\dot{m}_l(x) \tag{13}$$

The heat flux is used as the input data in this study. Therefore, it is convenient to use the relationship between the mass flow rates, $\dot{m}_v'(x)$ and $\dot{m}_l'(x)$, and the heat flux. Following Xu and Carey(1996), evaporation is only assumed to occur in the thin film. When steady state conditions are attained, the net mass flow rate of vapor at $x = L$ (the beginning point of thin film region, i.e. the junction of the thin film and meniscus regions) must be zero, i.e. $\dot{m}_v'(x_{\max}) = 0$. Therefore, for constant q'' , we have

$$\dot{m}_v(x) = \int_0^{x_{\max}-x} q''/h_{fg}\,dx, \qquad \dot{m}_l(x) = \int_0^x q''/h_{fg}\,dx \tag{14}$$

where h_{fg} is the latent heat of vaporization.

Boundary Conditions

The governing equation for the film thickness, Eq. (3), is a third-order nonlinear ordinary differential equation. Five prescribed boundary conditions for the film thickness, vapor and liquid pressures at $x = 0$ are as follows:

$$\delta\big|_{x=0} = \delta_0\,,\ \left.\frac{d\delta}{dx}\right|_{x=0} = 0\,,\ \left.\frac{d^2\delta}{dx^2}\right|_{x=0} = 0\,,\ P_{v,0} = P_{v,sat}(T_{v,0})\,,\ P_{l,0} = P_{v,0} - \frac{\overline{A}}{\delta_0^3} - \sigma K \tag{15}$$

Here the film thickness at $x = 0$, δ_o, is assumed to be 10^{-9} m. Water is used as the working fluid at a saturation temperature of 383 K, approximately.

Table1 Properties of working fluid

Properties	Values	Properties	Values
Dispersion constant ($\overline{A}$)	$2.87\text{x}10^{-21}$ J	Viscosity of liquid (μ_l)	$2.82\text{x}10^{-4}$ $\text{N}\cdot\text{s/m}^2$
Latent heat of evaporation (h_{fg})	$2.256\text{x}10^{6}$ J/kg	Density of vapor (ρ_v)	0.598 kg/m^3
Thermal conductivity of liquid (k_l)	0.68 $\text{W/m}\cdot\text{k}$	Viscosity of vapor(μ_v)	$12.02\text{x}10^{-6}$ $\text{N}\cdot\text{s/m}^2$
Density of liquid (ρ_l)	958.31 kg/m^3	Surface tension (σ)	$5.89\text{x}10^{-2}$ N/m

Numerical Procedures

To obtain the variation of thickness of thin film, we solve Eq. (3) with the boundary conditions, Eq. (15), using the 6th order Runge-Kutta method. Note that the length of thin film region (L), which is varied with some conditions, is calculated using the following procedure. The capillary force becomes a dominant force and the disjoining force can be neglected in the intrinsic meniscus region. Thus, we adopted the length when the value of $\overline{A}/\delta^3$ is much greater than or equal to that of σK as the length of thin film region. Once L was calculated, the film thickness at $x = L$, can be easily obtained.

RESULTS AND DISCUSSION

In this study, the flow and heat transfer characteristics for evaporation of water in thin film region of micro-channel are analyzed and the influence of heat flux is investigated numerically. Table 1 shows the basic properties of water as a working fluid.

Flow and Thermal Characteristics

In order to explain the flow characteristics in thin film, the non-dimensional film thickness (δ^*), the non-dimensional vapor pressure (P_v^*), and the non-dimensional liquid pressure (P_l^*) according to the non-dimensional channel length (x^*) are shown in Fig. 2(a), and the non-dimensional capillary and disjoining pressures (P_c^*, P_d^*) with x^* are shown in Fig. 2(b). The heat flux (q'') and the channel height (H) in Fig. 2 are 10^6 W/m^2 and 150 μm, respectively. The used non-dimensional parameters and their calculated values are listed in Table 2. In Fig.2, $x^* = 0$ and $x^* = 1$ denote the location of the beginning of thin film region (or the junction of the thin film region and the meniscus region) and the end of thin film region(or the beginning of the adsorbed region), respectively. It is can be seen in Fig. 2 (a) that the film thickness (δ^*), which has initially a maximum value of 8.22 μm, decreases sharply until $x^* = 0.6$ ($x = 4.9$ μm) and then it almost constant as the liquid flows. The film thickness is mainly influenced by

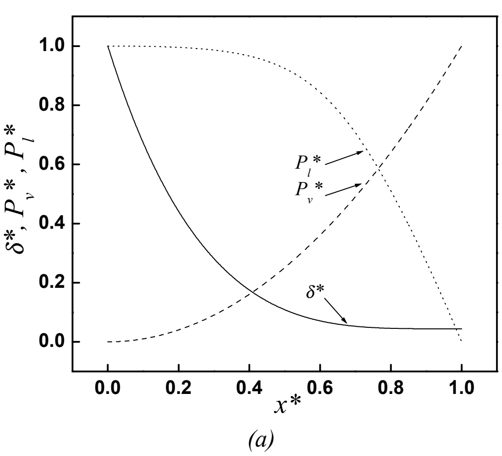

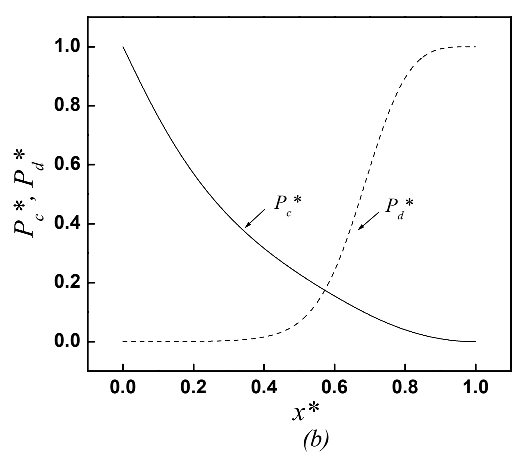

Fig. 2 (a) Dimensionless film thickness, vapor and liquid pressures and (b)capillary and disjoining pressures

Table 2 Non-dimensional parameters in Fig.2

Parameters	Calculated values	Parameters	Calculated values
$x^* = 1 - x/L$ $\delta^* = \delta / \delta_L$ $P_v^* = 1 - \dfrac{P_v - P_{v,0}}{P_{v,L} - P_{v,0}}$	L = 8.22 μm δ_L = 22.63 μm $P_{v,0}$ = 17,100 Pa $P_{v,L}$ = 17,099 Pa	$P_l^* = \dfrac{P_l - P_{l,0}}{P_{l,L} - P_{l,0}}$ $P_c^* = P_c / P_{c,L}$ $P_d^* = P_d / P_{d,0}$	$P_{l,0}$ = 26.947x10^5 Pa $P_{l,L}$ = 26.950x10^5 Pa $P_{c,L}$ = 246.35 Pa $P_{d,0}$ = 2.87x10^5 Pa

the vapor- and liquid -phase pressures. Thus, the variation of film thickness can be easily explained by a pressure distribution in the thin film region. The liquid pressure (P_l^*) with a maximum value of 26.95×10^5 Pa is not changed for $x^* < 0.4$, and then it decreases sharply until the end of thin film region. On the contrary, the vapor pressure (P_v^*) gradually increases with x^* and has a maximum value of 17,100 Pa at $x^* = 1.0$. The opposite pressure distribution, as shown in Fig. 2(a), means that the liquid and vapor flow reversely because for the both sides of liquid and vapor, the friction is interacted at the liquid-vapor interface as the liquid in thin film flows. Fig. 2(b) shows that the non-dimensional capillary pressure (P_c^*) decreases exponentially with x^* and its distribution has the same trend as that of the film thickness. But the disjoining pressure (P_d^*), which is not changed and has a minimum value for $x^* < 0.4$, increases sharply until $x^* = 0.8$ and then has a constant value until $x = 0$. It is also found that the flow in thin film region is dominantly affected by the disjoining pressure because its value is much greater than that of capillary pressure through all region of thin film as shown in Table 2 (i.e., the capillary and disjoining pressures at $x^* = 0$ have same values of 246.35 Pa and at $x^* = 1.0$ their values are 0 Pa and 2.87×10^5 Pa, respectively). Unfortunately, much research has neglected the effect of capillary pressure for the analysis of thin film region [Xu and Carey, and Ha and Peterson]. As it can be seen in Fig. 2(b) and Table 2, the capillary pressure plays a role in the flow characteristic in thin film region (i.e., $P_c = 0 \sim 246.35$ Pa) although its value is much smaller than that of disjoining pressure. Therefore, when the flow and heat transfer characteristics in the thin film region are analyzed numerically, the capillary pressure effect should be considered for more accurate results.

As mentioned earlier, many researches have paid attention to the analysis of heat and flow characteristics in thin film region. But most of them, the vapor pressure (P_v) was assumed to be constant for simplicity. To investigate the influence of the vapor pressure gradient, the film thickness along the flow direction for three cases (this study, $dP_v/dx = 10$, and $dP_v/dx = 0$) are shown in Fig. 3. Fig. 3 is the same conditions as Fig. 2 and new independent variable, z, which is defined as $z = L - x$, is introduced for convenient of the explanation. In this case, the length of thin film region, L, for three cases is the same value of 8.22 μm, which is the result of calculation in the case of considering the vapor pressure. As can be seen in this figure, in cases of the constant vapor pressure, $dP_v/dx = 0$, and the small pressure gradient, $dP_v/dx = 10$, the film thickness is underestimated compare to the result of this study. That is, the flow characteristic of thin film region is affected by the gradient of vapor pressure. Therefore, it is obvious that the vapor pressure should not be assumed to be constant when the flow characteristic is analyzed.

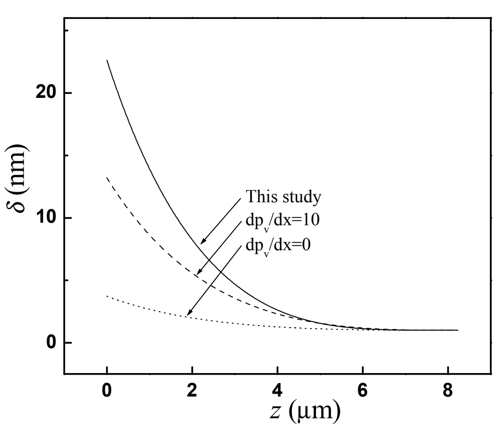

Fig. 3 The effect of gradient of vapor pressure on film thickness

Effect of Heat Flux

To explain the effect of input heat flux (q'') on the flow and heat transfer characteristics in the thin film region, we change the values of heat flux from 5×10^5 to 3×10^8 W/m^2. Fig. 4 presents the film thickness (δ) for various heat fluxes according to the flow direction, z . It can be seen that the increased heat flux decreases the film thickness and the length of thin film region, L , but it cannot change the shape of film thickness. To illustrate this result more clearly, the thin film length, the film thickness at $z=0$ ($x=L$), δ_L , and the evaporating mass flux, $\dot{m}''_{ev}$, for various heat fluxes are shown in Fig. 5. In this study, the evaporating mass flux can be related to the liquid mass flow rate by a mass balance and is defined as

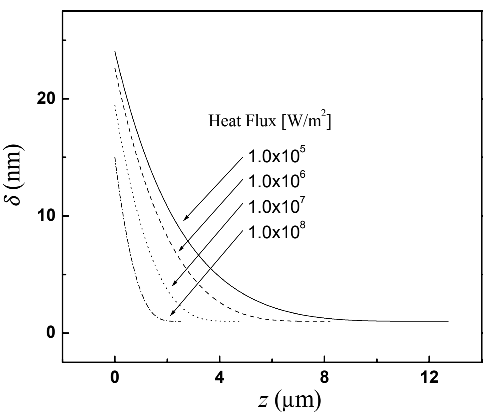

Fig. 4 Film thickness with heat flux

$$\dot{m}''_{ev} = -\frac{d\dot{m}_l(x)}{dx} \tag{16}$$

Note that the direction of evaporating mass flux is normal to the liquid-vapor interface. As shown in Fig. 5, as the heat flux increases, the length of thin film region, L , decreases sharply for $q''<10^7$ W/m^2 and then the decreasing rate is rather small and it finally approaches a constant value of 1.83 μm. That is, it is clear that the applied heat flux on the micro-channel doesn't influence the maximum length any more when its value is over 3×10^8 W/m^2. Fig. 5 also shows that the maximum film thickness, δ_L decreases exponentially with the heat flux and its variation has the same pattern as the maximum length. Above results have good agreements with Ha and Peterson's results (1996) qualitatively that the heat flux affects both the length of thin film and the film thickness. The decrease in length of thin film and maximum film thickness with the heat flux is mainly due to the increase in evaporative mass flux. The variation of evaporative mass flux can be also seen in Fig. 5 and the evaporative mass flux increases linearly as the heat flux increases. If the evaporative mass flux increases, the more liquid has to flow in the thin film region in order to maintain the law of mass conservation and the steady-state operation. It is clear that the increased evaporative mass flux results in the increase in gradient of liquid phase pressure.

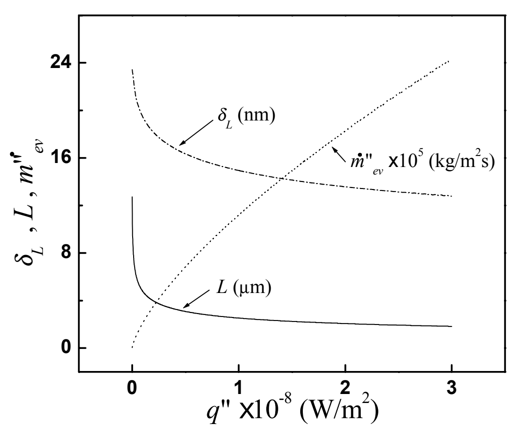

Fig. 5 Maximum lengths, maximum film thickness and evaporation mass flux with heat flux

To investigate the amount of heat transfer in micro-channel quantitatively, the average heat transfer coefficient, $\bar{h}$, is defined as

$$\bar{h} = \frac{1}{x}\int_0^x h(x)\,dx \approx \frac{1}{L}\int_0^L \frac{k_l}{\delta(x)}dx \tag{17}$$

Fig. 6 presents the average heat transfer coefficient with the heat flux. As the heat flux increases, the average heat transfer coefficient which is defined in Eq. (17) increases. As stated earlier, the increased heat flux cause to increase the amount of evaporation at the liquid-vapor interface and the increased amount of evaporation brings on the decrease in film thickness and length of thin film region simultaneously. Therefore, the decrease in film thickness will decrease the thermal resistance in thin film region and cause to increase the heat transfer.

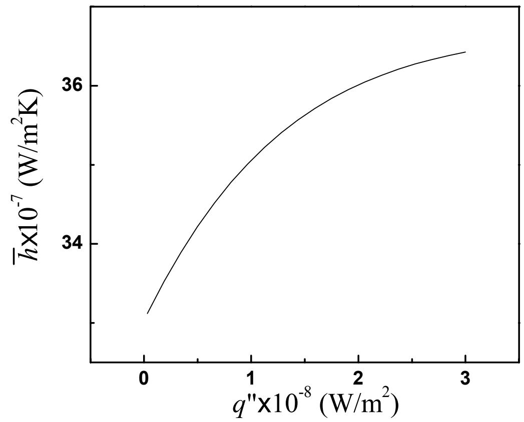

Fig. 6 Average heat transfer coefficient with heat flux

CONCLUSIONS

A mathematical model considering the vapor pressure as well as liquid pressure is presented in order to analyze the two-phase flow and heat transfer phenomena in a thin film region of micro channel. Using the model, the effects of the heat flux on the flow and thermal characteristics are investigated. The results show that the shape and thickness of thin film in micro-channel is influenced by the vapor phase pressure as well as the liquid phase pressure. In analyzing the thin film region, the capillary force must be considered although its value is rather small compare to the disjoining pressure. The disjoining pressure is still the dominant driving force in this region. The disjoining pressure increases sharply from the location of 40% of thin film region. As the heat flux increases, the length of thin film region and the maximum thickness decrease exponentially and the local evaporation mass flux linearly increases because of the increasing in pressure difference between liquid and vapor pressures. It is always not guaranteed that the thin film length is shortened as the heat flux is increased.

ACKNOWLEDGEMENTS

This research was supported by The Center of Innovative Design Optimization Technology, Korea Science and Engineering Foundation.

REFERENCES

Derjaguin, B.V., Nerpin, S.V., and Churaev, N.V., “Effect of Film Transfer upon Evaporating Liquids from Capillaries”, RILEM Bulletin, vol. 29, no. 1, pp. 93-98, 1965.

Ha, J.M. and Peterson, G.P., “ The Interline Heat Transfer of Evaporating Thin Film Along a Micro Grooved Surface”, *ASME J. of Heat Transfer*, vol. 118, pp. 747-755, 1996.

Khrustalev, D. and Faghri, A., “Thick-Film Phenomenon in High-Heat-Flux Evaporation From Cylindrical Pores”, ASME J. of Heat Transfer, vol. 119, pp. 272-278, 1997.

Kobayashi, Y., Ikeda, S., and Iwasa, M., “ Evaporative heat Transfer at the Evaporative Section of a Grooved Heat Pipe”, J. of Thermophysics and Heat Transfer, vol. 10, no. 1, pp. 83-89, 1996.

Mirzamoghadam, A. and Catton, I., " A Physical Model of the Evaporating Meniscus", ASME J. of Heat Transfer, vol. 110, pp. 201-207, 1988.

Potash, M., Jr., and Wayner, P.C. Jr., "Evaporation from a Two-Dimensional Extended Meniscus", Int. J. of Heat and Mass Transfer, vol. 15, pp. 1851-1863, 1972.

Schonberg, J. and Wayner, P.C. Jr., “ An Analytical Solution for the Integral Contact Line Evaporative Heat Sink”, AIAA *J. of Thermophysics and Heat Transfer*, vol. 6, no.1, 128-134, 1992.

Swanson, L.W. and Herdt, G.C., " Model of the Evaporating Meniscus in a Capillary Tube", ASME J. of Heat Transfer, vol. 114, pp. 434-441, 1992.

Wayner, P.C. Jr., "Long Range Intermolecular Forces in Change-of-Phase Heat Transfer", *33rd National Heat Transfer Conference*, pp. 1-16, NHTC99-320, Albuquerque, Mexico, 1999.

Xu, X, and Carey, V.P., “Film Evaporation from a Micro-Grooved Surface-An Approximate Heat Transfer Model and its Comparison with Experimental Data”, *AIAA J. of Thermophysics and Heat Transfer*, vol. 4, no. 4, pp. 512-520, 1990.